ALCOHOLISM CLINICAL & EXPERIMENTAL RESEARCH

Adolescent Intermittent Alcohol Exposure: Persistence of Structural and Functional Hippocampal Abnormalities into Adulthood

Mary-Louise Risher, Rebekah L. Fleming, W. Christopher Risher, K. M. Miller, Rebecca C. Klein, Tiffany Wills, Shawn K. Acheson, Scott D. Moore, Wilkie A. Wilson, Cagla Eroglu, and H. S. Swartzwelder

Background: Human adolescence is a crucial stage of neurological development during which ethanol (EtOH) consumption is often at its highest. Alcohol abuse during adolescence may render individuals at heightened risk for subsequent alcohol abuse disorders, cognitive dysfunction, or other neurological impairments by irreversibly altering long-term brain function. To test this possibility, we modeled adolescent alcohol abuse (i.e., intermittent EtOH exposure during adolescence [AIE]) in rats to determine whether adolescent exposure to alcohol leads to long-term structural and functional changes that are manifested in adult neuronal circuitry.

Methods: We specifically focused on hippocampal area CA1, a brain region associated with learning and memory. Using electrophysiological, immunohistochemical, and neuroanatomical approaches, we measured post-AIE changes in synaptic plasticity, dendritic spine morphology, and synaptic structure in adulthood.

Results: We found that AIE-pretreated adult rats manifest robust long-term potentiation, induced at stimulus intensities lower than those required in controls, suggesting a state of enhanced synaptic plasticity. Moreover, AIE resulted in an increased number of dendritic spines with characteristics typical of immaturity. Immunohistochemistry-based analysis of synaptic structures indicated a significant decrease in the number of co-localized pre- and postsynaptic puncta. This decrease is driven by an overall decrease in 2 postsynaptic density proteins, PSD-95 and SAP102.

Conclusions: Taken together, these findings reveal that repeated alcohol exposure during adolescence results in enduring structural and functional abnormalities in the hippocampus. These synaptic changes in the hippocampal circuits may help to explain learning-related behavioral changes in adult animals preexposed to AIE.

Key Words: Hippocampus, Long-Term Potentiation, Dendritic Spines, Adolescence, Ethanol.

ADOLESCENCE IS A critical period for cognitive, emotional, and social maturation (Choudhury et al., 2006) that is accompanied by the pruning of synapses, refinement of neural circuitry, and changes in receptor expression and sensitivity (Kilb, 2012). These processes contribute to the normal maturation of cognitive processes crucial for successful adult function, including planning, inhibitory control, and working memory (Paus, 2005).

Adolescence is also a period during which alcohol consumption is often initiated and sustained at high levels (Squeglia et al., 2012). While it has become clear that adolescents respond differently than adults to the acute effects of ethanol (EtOH) on learning, sedation, and motor function (Little et al., 1996; Markwiese et al., 1998; Spear, 2000), the enduring consequences of repeated EtOH exposure during this developmental period have only recently begun to be addressed.

In humans, chronic excessive alcohol use during adolescence has been associated with cognitive deficits manifesting in adulthood, particularly in the domain of memory function (Brown et al., 2000; Hanson et al., 2011). In animal models used to reflect human levels of consumption, behavioral studies have shown that adolescent intermittent EtOH (AIE) exposure in rats results in long-lasting changes in EtOH sensitivity, consumption, and aversion (Diaz-Granados and Graham, 2007; Matthews et al., 2008; Risher et al., 2013). With respect to learning and memory in particular, it has been reported that AIE, but not chronic intermittent EtOH (CIE)

From the Durham VA Medical Center (M-LR, RLF, KM, RK, SKA, SDM, WAW, HSS), Duke University Medical Center, Durham, North Carolina; Department of Psychiatry and Behavioral Sciences (M-LR, RLF, KM, RK, SKA, SDM, HSS), Duke University Medical Center, Durham, North Carolina; Department of Cell Biology (WCR, CE), Duke University Medical Center, Durham, North Carolina; Department of Molecular Physiology & Biophysics (TW), Vanderbilt University, Nashville, Tennessee; Social Sciences Research Institute (WAW), Duke University Medical Center, Durham, North Carolina; and Department of Psychology and Neuroscience (HSS), Duke University Medical Center, Durham, North Carolina.

Received for publication February 2, 2015; accepted March 12, 2015.

Reprint requests: H. Scott Swartzwelder, Department of Psychiatry and Behavioral Sciences, Duke University Medical Center and Durham VA Medical Center, Building 15, VAMC, 508 Fulton Street, Durham, NC 27705; Tel.: 919-971-0964; Fax: 919-286-6811; E-mail: hss@duke.edu

DOI: 10.1111/acer.12725

exposure in adulthood, results in greater sensitivity to the spatial memory-impairing effects of acute EtOH in the radial arm maze, in the absence of an effect on baseline learning ability (Risher et al., 2013; White et al., 2000). Interestingly, AIE has also been shown to reduce the efficacy of EtOH to impair spatial learning in the Morris water maze 24 hours after the last EtOH dose (Silvers et al., 2003, 2006), although it is noteworthy that the effect may have been driven by withdrawal, tolerance, or both, given the brief delay between repeated EtOH exposure and testing. Aside from the subsequent responsiveness to EtOH challenge, Sircar and Sircar (2005) reported that AIE caused deficits in Morris water maze performance up to 25 days after the last EtOH treatment, and fear retention deficits have also been observed 25 days following AIE exposure (Broadwater and Spear, 2013).

At the neuronal level in similar AIE rodent models (which achieve equivalent blood EtOH concentrations [BECs]), enduring functional effects are produced that are not apparent when comparable EtOH exposure is administered in adulthood. For example, AIE has been shown to reduce A-type potassium current (I_A) in GABAergic hippocampal interneurons (Li et al., 2013), $GABA_A$ receptor-mediated tonic current in dentate granule cells (Fleming et al., 2012, 2013) in adulthood, and protein levels of delta and alpha-4 GABA receptors in whole hippocampus (Centanni et al., 2014), while comparable EtOH exposure during adulthood did not produce equivalent long-lasting changes in these cellular functions or receptor proteins. Thus, not only does adolescent EtOH exposure promote long-lasting changes in hippocampal cellular function, but that adolescence is also a period of distinctive vulnerability to the long-term effects of EtOH, enduring even after an extended period of abstinence.

While these findings support heightened vulnerability to the long-term consequences of repeated alcohol exposure during adolescence, the extent to which AIE alters subsequent hippocampal neuronal, synaptic, and behavioral processes is unclear. We used hippocampal slices to assess the long-term effects of AIE (an established model of intermittent EtOH exposure) on CA1 structure and function. The CA1 area of the hippocampus was selected because of its role in learning/memory processes and because it has been a focus of studies in the emerging literature on the enduring effects of AIE. Here, we assessed the effects of AIE on long-term potentiation (LTP), dendritic spine morphology (to determine whether AIE alters synaptic structure that in turn can influence synaptic function), and postsynaptic density proteins; the latter of which has been found to influence dendritic spine morphology and play a critical role in the recruitment and stabilization of excitatory synapses and synaptic function (Béïque et al., 2006; El-Husseini et al., 2000; Zheng et al., 2012). This approach represents a comprehensive analysis combining physiological, biochemical, and morphological assessments that support the hypothesis that AIE results in neuronal changes that persist into adulthood, emphasizing the vulnerability of this critical developmental period to insults that can potentially alter the trajectory of brain development.

MATERIALS AND METHODS

All of the procedures used in this study were conducted in accordance with the guidelines of the American Association for the Accreditation of Laboratory Animal Care and the National Research Council's Guide for Care and Use of Laboratory Animals and were approved by the Durham VA Medical Center and the Duke University IACUCs.

Male postnatal day (PND) 25 Sprague-Dawley rats (Charles River, Raleigh, NC) were double housed and maintained in a temperature- and humidity-controlled room with ad libitum access to food and water. Animals were dosed using modified methods previously described (Risher et al., 2013). Briefly, animals were allowed to acclimatize for 5 days on a reverse 12-hour:12-hour light:dark cycle (lights off at 9:00 AM) prior to beginning AIE or saline administration. All animals were exposed to AIE or saline beginning on PND 30 and consisting of 10 doses of 5 g/kg EtOH (35% v/v in saline at 18.12 ml/kg; VWR, Suwanee, GA) or isovolumetric saline administered by intragastric gavage (i.g.) using a 2 days on, 1 day off, 2 days on, and 2 days off intermittent schedule for 16 days, followed by a 24- to 29-day washout period, thus allowing all animals to reach adulthood prior to sacrifice. EtOH doses were selected to produce BECs that are consistent with adolescent human BECs during binge drinking episodes.

Blood EtOH Concentration

To avoid the possible confounds associated with stress and stress/EtOH interactions in experimental animals, a group of animals ($n = 7$) were dosed in parallel with the electrophysiology animals to assess BECs during the intermittent EtOH administration. Animals were dosed (i.g.) on the intermittent schedule described above with 5 g/kg EtOH (35% v/v in normal saline) beginning on PND 30. Approximately 150 μl of blood was drawn from the lateral saphenous vein at 60 minutes post-EtOH administration on the first and last day of administration. Serum was collected from centrifuged samples and stored at −80°C. Samples were analyzed in triplicate using an Analox GL5 alcohol analyzer (Analox Instruments, Lunenburg, MA).

Electrophysiology

Twelve rats exposed to AIE and 12 controls were used for these electrophysiological experiments. Extracellular field recordings were performed in the CA1 area of hippocampal slices using modified techniques described previously (Bourne and Harris, 2011; Klein et al., 2014; Swartzwelder et al., 1995). Briefly, rats (PND 70 to 75) were anesthetized with isoflurane, decapitated, and the brain quickly removed. One hemisphere was randomly selected and prepared for Golgi-Cox staining (as described in a later section), while the other hemisphere was placed in ice-cold artificial cerebral spinal fluid (aCSF) consisting of (in mM) 116.4 NaCl, 5.4 KCl, 1 NaH_2PO_4, 26.2 $NaHCO_3$, 10 D-glucose, 3.2 $CaCl_2$, 1.6 $MgSO_4$ and bubbled with a gas mixture of 95% O_2 to 5% CO_2. Coronal sections (400 μm) were cut using a vibratome and incubated at room temperature for 15 minutes. Slices were then transferred to a holding chamber and maintained at 30°C for a minimum of 90 minutes prior to recording. Slices were maintained at 30°C in the recording chamber and perfused with aCSF at a flow rate of 4 ml/min. A glass micropipette (recording tip 2 μm, 2 to 4 MΩ containing 120 mM NaCl) was placed in the CA1 *stratum radiatum* and field excitatory postsynaptic potentials (fEPSPs) were elicited by stimulating the Schaffer collateral fibers with a concentric bipolar electrode (FHC, Bowdoin, ME). An Axopatch 200B amplifier (10 kHz low-pass filter) and pClamp software (Sunnyvale, CA, RRID: rid_000085, 10 kHz sampling rate) were used to record all data. Input/output curves were generated in all slices, and the subsequent baseline stim-

ulus intensity was set at a level that elicited 40% of maximal fEPSP slope. Baseline fEPSPs were recorded every 60 seconds for 25 minutes and LTP was induced using a theta burst stimulation (TBS) protocol consisting of 2 stimulus trains, each consisting of ten 4-pulse 100 Hz bursts with a 200-ms interburst interval. The stimulus trains were delivered 30 seconds apart, at a stimulus intensity of 20, 30, or 40% of maximal fEPSP slope. fEPSPs were then evoked with baseline level stimulus pulses every 60 seconds for 60 minutes (n = 8 to 12/treatment group). LTP was defined as >15% potentiation 60 minutes after TBS induction. Any slices that failed to maintain a stable baseline (more than ± 5% of baseline for 5 consecutive time points) were removed from the analysis.

Golgi-Cox Staining

Rats were handled and dosed with EtOH or saline as described above (n = 5 per treatment group). Following the 24- to 29-day washout period, Golgi-Cox staining was performed as previously described (Risher et al., 2014). The animals (PND 70 to 75) were deeply anesthetized with isoflurane, decapitated, and the brain was quickly removed. One hemisphere was randomly selected, quickly rinsed in distilled water, and immersed in a 1:1 mixture of solutions A and B (Rapid Golgi Stain Kit; FD Neurotechnologies, Baltimore, MD). The other hemisphere was placed in ice-cold aCSF in preparation for electrophysiology (as described above). After 2 weeks of impregnation in solutions A and B, brains were transferred to solution C for 48 hours, then removed and frozen in tissue freezing medium (Electron Microscopy Sciences, Hatfield, PA). Coronal slices (100 μm) were sectioned using a cryostat (Microm HM 505E; ThermoFisher Scientific, Waltham, MA) and mounted onto 2% gelatin-coated slides (LabScientific Inc., Livingston, NJ). Sections were stained with a mixture containing solutions D and E, dehydrated, cleared, and coverslipped with Permount.

Dendritic Spine Analysis. Golgi-impregnated neurons were visualized using the Neurolucida system (MBF Bioscience, Williston, VT, RRID: nif-000-10382), and image stacks were generated using a 100× oil immersion lens. Each image stack was extracted using ImageJ software (NIH, Bethesda, MD) and subsequently imported into RECONSTRUCT software (available from http://synapses.clm.utexas.edu/tools/index.stm; Fiala, 2005) for analysis as described in Risher and colleagues (2014) with modifications. Briefly, secondary and tertiary dendritic branches of CA1 hippocampal neurons were analyzed using an unbiased rating system by measuring the length and width of each protrusion with visible connections to the dendritic shaft from dendritic segments 10 μm in length. Average spine densities were calculated using 2 to 3 separate dendrites from at least 4 to 5 separate image stacks per animal. Spine types were determined on the basis of the ratio of the width (W) of the spine head to the length (L) of the spine neck and classified as (in μm): filopodia (L > 1.5), thin/long thin (L < 1.5 & L:W > 1), stubby (L:W < 1), and mushroom (W > 0.6), also see Fig. 2*B* (Klein et al., 2014; Risher et al., 2014).

Dendritic Branching Analysis. Analysis was performed using a Neurolucida system and NeuroExplorer: Neurophysiological Data Analysis Package (MBF Bioscience, Williston, VT, RRID: nif-000-10382). Neurons were visualized using a 40× oil immersion lens. CA1 hippocampal neurons that were clearly visible and not severed in the sectioning and mounting process were randomly selected and traced, taking into account both the length and width of all discernible dendritic branches. Final calculations for dendritic branch number, length, and Sholl analysis were made from Neurolucida-derived numerical measurements based on 3 dendrite tracings per animal. All Golgi-Cox images were prepared using a custom MATLAB code (available from c.eroglu@cellbio.duke.edu upon request).

Immunohistochemistry

To probe for changes in the number of structurally mature synapses, VGlut1 was used as a presynaptic marker, and 2 members of the postsynaptic membrane-associated guanylate kinases (MAGUKs) family, the postsynaptic density protein-95 (PSD-95) and synapse-associated protein 102 (SAP102), were used to identify the postsynaptic partners. Rats were handled and dosed with AIE or saline as described above (n = 5 per treatment group). Immunohistochemistry was performed as previously described in Ippolito and Eroglu (2010) with modifications. Primary (guinea pig anti-VGlut1, EMD Millipore, Billerica, MA, cat#AB5905, RRID: AB_2301751; rabbit anti-PSD-95, Invitrogen, Life Technologies, Grand Island, NY, cat#51-6900, RRID:AB_87705; and rabbit anti-SAP102, Abcam, Cambridge, MA, cat#ab3438, RRID: AB_303802) and secondary antibodies (goat anti-guinea pig IgG 488 Alexa Fluor, Life Technologies, cat#A11073, RRID: AB_142018 and goat anti-rabbit IgG 594 Alexa Fluor, Life Technologies, cat#A11012, RRID:AB_141359) were prepared in 5% normal goat serum, 0.2% triton in Tris-buffered saline solution. Rats (PND 70) were deeply anesthetized with isoflurane and transcardially perfused with phosphate-buffered saline (PBS), pH 7.4, containing 25 U/ml heparin, followed by 4% paraformaldehyde in PBS. Brains were removed and postfixed for 24 hours at 4°C in 4% paraformaldehyde in PBS. The brains were rinsed in PBS and placed in 30% sucrose in PBS. Upon sinking, brains were removed and frozen in tissue freezing medium (Electron Microscopy Sciences, Hatfield, PA) and stored at −80°C. Sagittal sections (20 μm) were cut using the Leica CM 3000 (Leica Microsystems, Buffalo Grove, IL) and placed in glycerol:Tris-buffered saline solution. Glycerol was removed and slices were blocked with 5% normal goat serum, 0.2% triton for 1 hour at room temperature. Slices were incubated in primary antibodies for 3 days at 4°C, followed by secondary antibodies for 2 hours at room temperature. Sections were rinsed and coverslipped with Vectashield mounting media (Vector Laboratories, Burlingame, CA). Confocal z-stacks (5 μm thick, optical section depth 0.33 μm, 15 sections/z-stack, 1,024 × 1,024 image size) of the synaptic zone in area CA1 were imaged at 63× magnification on a Leica SP5 confocal laser-scanning microscope. Maximum projections of 3 consecutive optical sections (corresponding to 1 μm total depth) were generated from the original z-stack. The Puncta Analyzer plugin (available upon request from c.eroglu@cellbio.duke.edu) for ImageJ was used to count the number of co-localized, pre- and postsynaptic puncta (Ippolito and Eroglu, 2010).

Statistical Analysis

Comparisons between treatments were made using independent-samples Student's t-tests for Golgi-Cox and immunohistochemistry. Analysis of covariance was used for the Sholl analysis. Repeated measures analysis of variance and independent-samples Student's t-tests were used for analysis of electrophysiological data. Degrees of freedom were corrected using the Greenhouse-Geisser procedure where the assumption of sphericity was not met. All analyses were conducted using SPSS (v.21/22; Chicago, IL, RRID: rid_000042). Statistical significance was assessed using an alpha level of 0.05. All data are presented in figures as the mean ± SEM.

RESULTS

Blood EtOH Concentrations

We assessed BECs to confirm blood EtOH levels consistent with those observed during human drinking episodes.

Animals that received 5 g/kg EtOH achieved average BECs (in mg/dl ± SEM) of 199.7 ± 19.9 sixty minutes after the first dose and 172.8 ± 13.3 sixty minutes after the last dose. These BECs are consistent with those in our previous studies (Acheson et al., 2012) and achieved by adolescent humans during binge drinking episodes (NIAAA, 2004).

Elevated Propensity for LTP Induction After AIE

Prior to inducing LTP, we assessed whether AIE influenced the baseline stimulation/response–input/output (I/O) curves; an indication of AMPA receptor function. We found that AIE had no effect on the I/O curve prior to TBS ($p = 0.237$), suggesting that AIE does not appreciably alter fast excitatory synaptic transmission driven by AMPA receptor function (Fig. 1*C*). Assessment of LTP after low intensity TBS (20% of maximum fEPSP slope) showed that potentiation was elicited in both AIE and saline-treated animals over the first 4 minutes (control: 121.67% ± 2.33 and AIE: 130.92 ± 1.98; Fig. 1*D*). This potentiation rapidly decayed in saline control slices but persisted for 60 minutes in slices from AIE animals, thus reaching criteria for LTP (>15% potentiation 60 minutes after TBS induction). However, following strong TBS trains (40% and 30% maximum

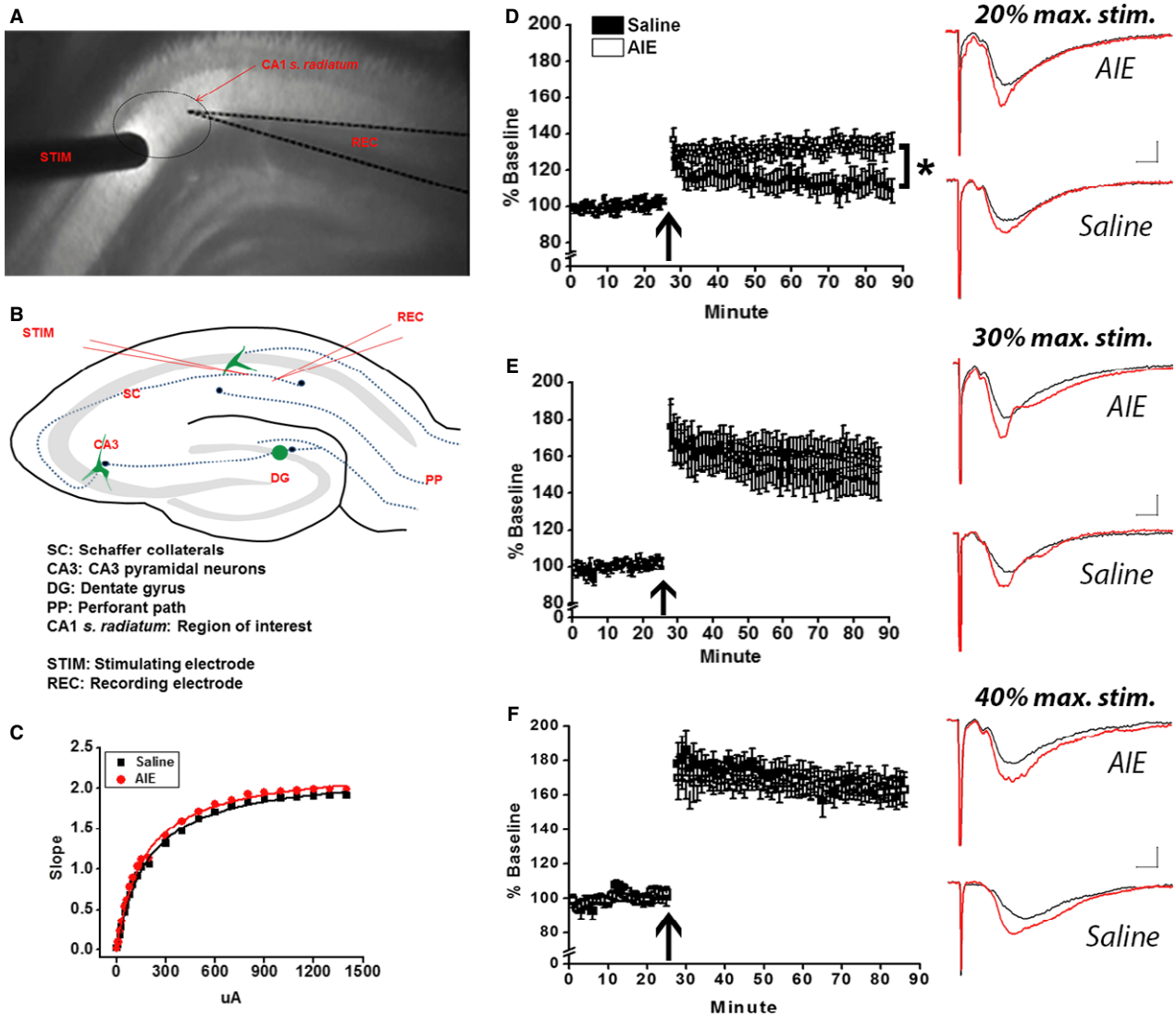

Fig. 1. Adolescent intermittent ethanol (AIE) increases the propensity for long-term potentiation (LTP) induction in adulthood**.** Representative image of a typical hippocampal slice showing the location of the STIM (stimulating electrode) and the REC (recording electrode) within CA1 (**A**). Schematic of the hippocampal slice showing the major pathways projecting throughout the slice in relation to the STIM and REC (**B**). The fEPSP slope was plotted against stimulus intensity to generate input/output curves for AIE- and saline-treated animals, $F(1, 68) = 501.879$, $p = 0.474$ (**C**). Time course of the averaged initial fEPSP slope during 25 minutes baseline and after 20% theta burst stimulation (TBS) (**D**). Saline-treated animals (filled squares) failed to maintain their potentiated state beyond 4 minutes post-TBS, while AIE animals (open squares) maintained their potentiated state throughout the 60 minutes, thus meeting our criteria for LTP, $F(1, 19) = 946.079$, $^*p = 0.045$). Thirty percent TBS (**E**) and 40% TBS (**F**) protocols elicited robust, stable LTP in saline (filled squares)- and AIE (open squares)-treated animals , $F(1, 21) = 581.748$, $p = 0.542$, and $F(1, 16) = 1{,}240.989$, $p = 0.596$, analysis of variance, respectively. Arrows indicate onset of TBS. Representative images of pre- and post-TBS accompany all quantified data; black lines indicate pre-TBS traces, while red lines indicate post-TBS traces (far right panel). $^*p < 0.05$, $n = 8$ to 12 animals/treatment.

fEPSP slope), robust LTP was observed in slices from both AIE and saline control animals, with no AIE-dependent change in the magnitude of LTP (Fig. 1*E,F*). These data show that AIE results in an elevated propensity for LTP induction by low intensity TBS in adulthood, suggesting that AIE induces a hyperplastic state in hippocampal circuits, which could interfere with further memory acquisition due to enhanced metaplasticity (Brun et al., 2001; Moser et al., 1998).

AIE Increased the Number of Immature Dendritic Spines and Decreased the Number of Mature Dendritic Spines in Area CA1 in Adulthood

Dendritic spine density and structural diversity are useful indices of excitatory synapse number and maturity, respectively (Bourne and Harris, 2007, 2008; Matsuzaki, 2007). Therefore, in order to determine whether changes in spine morphology could contribute to the changes in LTP threshold observed after AIE, we conducted Golgi-Cox staining of area CA1. We categorized and assessed 4 spine types representing stages of maturation throughout the life of the spine: mushroom and stubby spines, generally considered to be mature; thin/long spines with smaller spine heads, which represent the more intermediate to immature spine types; and filopodia-like structures, which are considered to be the most immature phenotype and are highly expressed during development (representative images are shown in Fig. 2*A,C*). Given the increase in functional plasticity that we observed in the LTP experiment, we hypothesized that AIE would induce an increase in immature spine morphology in adulthood that may contribute to the adolescent-like threshold for LTP.

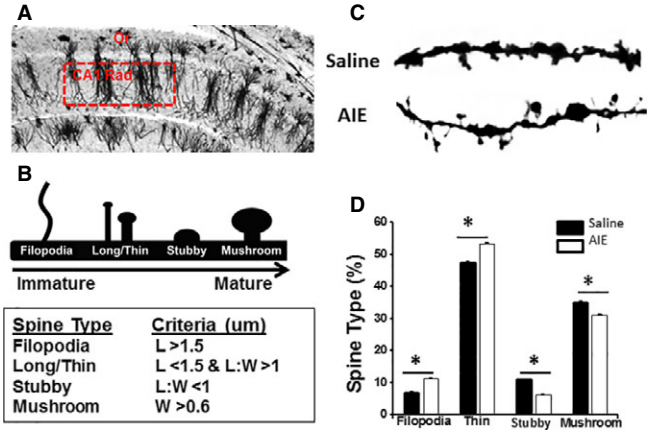

Fig. 2. Adolescent intermittent ethanol (AIE) results in an immature-like dendritic spine phenotype in adulthood. Representative image of Golgi-Cox staining within CA1. Or = *stratum oriens*, CA1 s. rad = *stratum radiatum* (**A**). Examples of the dendritic spine types analyzed (from left to right): filopodia, thin/long thin, stubby, and mushroom; the criteria for each spine type are listed (**B**). Representative images of saline- and AIE-treated dendritic sections (**C**). Quantification of spine type (**D**). Independent *t*-tests showed a significant difference in spine type with AIE promoting the development of more immature spines and less mature spines when compared to controls: $*p < 0.001$, filopodia and stubby; $p = 0.017$, mushroom; $p = 0.041$, long thin; 10 to 15 samples per animal (*t*-test), $*p < 0.05$, $n = 5$ animals/treatment.

As predicted, AIE resulted in a shift toward a greater proportion of immature spines in adulthood. Specifically, we observed an increase in filopodia (6.87% ± 0.01 vs. 11.36% ± 0.01, saline vs. AIE) and long/thin spines (47.15% ± 0.03 vs. 51.37% ± 0.031, saline vs. AIE) and a decrease in the number of stubby (10.93% ± 0.014 vs. 6.18% ± 0.01) and mushroom spines (35.04% ± 0.02 vs. 31.09% ± 0.017) (Fig. 2*C,D*). In addition, AIE subtly but significantly increased the length of all spine types (overall length [in μm] saline: 0.8857 ± 0.0159; AIE: 0.9238 ± 0.0148; $t(842) = -1.758$, $p = 0.04$). Despite the significant changes in spine type and length, AIE had no effect on overall spine width or density (data not shown). Thus, AIE drives a shift in spine type toward an immature phenotype, and taken together with our functional analysis, these findings indicate that AIE leads to enhanced structural and functional plasticity within CA1 neuronal circuitry.

AIE Reduces Postsynaptic Proteins (PSD) in CA1 Neurons

The presence of immature-like dendritic spines after AIE suggests alteration of postsynaptic features (Tada and Sheng, 2006). Therefore, we assessed changes in the abundance of a member of the postsynaptic MAGUKs family, the PSD-95. We chose PSD-95 because it is known to have mechanistic influence over postsynaptic stability, excitatory receptor insertion (Béïque et al., 2006; Zheng et al., 2012), and spine morphology (El-Husseini et al., 2000).

Using immunohistochemistry, we determined that AIE reduced the punctate PSD-95 staining in the CA1 region of the hippocampus, $t(27) = 2.249$, $p = 0.017$ (Fig. 3*B,E*), driving a decrease in co-localized PSD-95/VGlut1 puncta, $t(27) = 2.385$, $p = 0.012$ (Fig. 3*B,C*) in the absence of an effect on presynaptic VGlut1, $t(27) = 1.604$, $p = 0.06$ (Fig. 3*B,D*). These data suggest that AIE not only enhances the induction of hippocampal synaptic plasticity, but may do so through sustaining the presence of immature synapses into adulthood, as reflected by an increase in immature dendritic spines and a reduction in PSD-95. To explore this, further, we assessed SAP102, which is also a MAGUK postsynaptic protein that interacts with a multitude of membrane and cytoplasmic proteins including the NR2 subunit, the same region that is required for the localization of excitatory receptor subunits to the PSD (Yuste, 2009). SAP102 was chosen because it is highly expressed in immature spines (relative to mature spines) and has been shown to not only compensate for a loss of PSD-95 but also to be involved in excitatory receptor subunit trafficking and clustering (Elias et al., 2008).

Using immunohistochemistry, we determined that AIE actually reduced the number of co-localized SAP102/VGlut1 puncta, $t(27) = 2.363$, $p = 0.013$ (Fig. 4*A,B*), which was driven by a reduction in SAP102 puncta, $t(27) = 2.826$, $p = 0.004$ (Fig. 4*A,D*) as no changes in presynaptic VGlut1

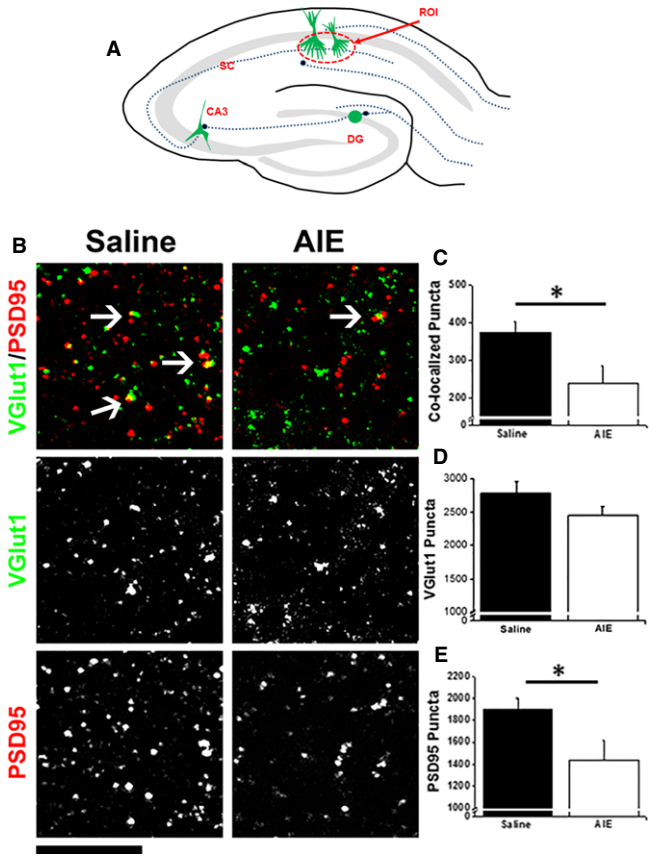

Fig. 3. Adolescent intermittent ethanol (AIE) reduces co-localized pre- and postsynaptic VGlut1/PSD-95 in adulthood. Schematic of a hippocampal slice showing the major projecting pathways in relation to the region of interest (ROI) in CA1 (**A**). Representative images of immunolabeling of CA1 hippocampal neurons in control and AIE animals for pre-(VGlut1) and post-(PSD-95) (**B**) synaptic markers. Arrows indicate yellow co-localized pre-(VGlut1) and post-(PSD-95) synaptic puncta. AIE significantly decreased co-localized pre- and postsynaptic puncta (*$p = 0.012$, *t*-test) (**C**), indicative of a decrease in synapse formation. This co-localization was unaffected by the number of VGlut1 puncta staining after AIE ($p = 0.06$, *t*-test) (**D**) but rather was influenced by a significant decrease in the number of PSD-95 puncta (*$p = 0.017$, *t*-test) (**E**). Three image stacks/animal and $n = 5$ animals/treatment, *$p < 0.05$. Scale bar represents 10 μm.

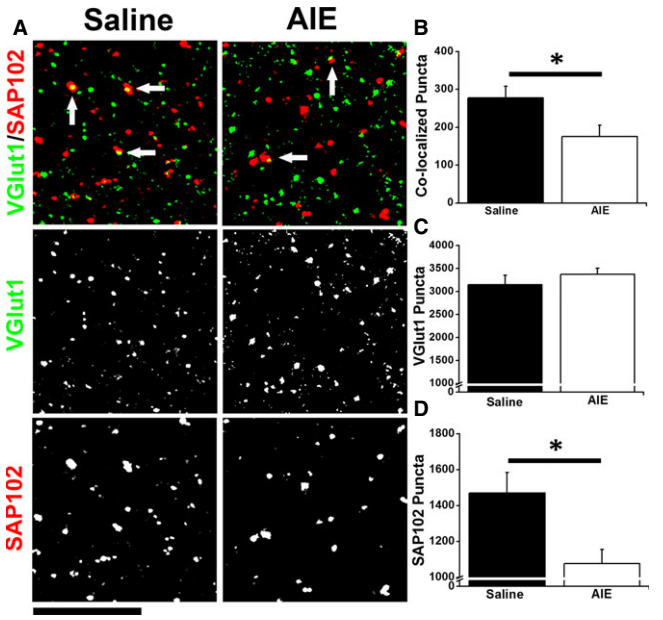

Fig. 4. Adolescent intermittent ethanol (AIE) reduces co-localized pre- and postsynaptic VGlut1/SAP102 in adulthood. Representative images of immunolabeling of CA1 hippocampal neurons in control and AIE animals for pre-(VGlut1) and post-(SAP102) (**A**) synaptic markers. Arrows indicate yellow co-localized pre-(VGlut1) and post-(SAP102) puncta. AIE significantly decreased co-localized pre- and postsynaptic puncta (*$p = 0.013$, *t*-test) (**B**). This co-localization was unaffected by the number of presynaptic VGlut1 puncta staining after AIE ($p = 0.19$, *t*-test) (**C**) but rather was influenced by a significant decrease in the number of postsynaptic SAP102 puncta (*$p = 0.005$, *t*-test) (**D**). Three image stacks/animal and $n = 5$ animals/treatment, *$p < 0.05$. Scale bar represents 10 μm.

were observed, $t(27) = 2.410$, $p = 0.186$ (Fig. 4*A,C*). Thus, after AIE, SAP102 is not increased as would be expected in immature spines, and SAP102 is not elevated to compensate for a loss of PSD-95, indicating that the changes in LTP and spine morphology may indicate spine/neuronal pathology rather than immaturity per se. Nevertheless, these results demonstrate that AIE results in significant reduction in the co-localized pre- and postsynaptic proteins (VGlut1 and PSD-95 or SAP102) indicating a significant change in the synaptic structures as a long-term consequence of AIE.

AIE Does Not Produce Changes in Gross Dendritic Morphology

Although the AIE-induced decrease in PSD-95 and SAP102 puncta does not appear to be due to a decrease in spine density (Fig. 2), it is possible that a decrease in overall dendritic branching or overall dendritic number could drive the decrease in PSD-95 and SAP102 within CA1 (i.e., fewer branches = fewer synapses). Therefore, we assessed changes in dendritic branch number and length and conducted a Sholl analysis. There was no significant change in the Sholl analysis, $F(1, 1{,}076) = 0.249$, $p = 0.618$ (Fig. 5), dendritic branch length/total outgrowth, $t(22) = 0.168$, $p = 0.434$, or branch number, $t(22) = 1.18$, $p = 0.126$ (Fig. 5), suggesting that gross changes in neuronal morphology are not driving the changes in PSD-95 and SAP102 puncta observed in Figs 3 and 4.

DISCUSSION

The long-term impact of repeated EtOH exposure during adolescence has become a topic of intensive interest and recent investigation. Because EtOH is well known to affect memory and hippocampal function, and to do so more potently during adolescence than adulthood (Spear and Swartzwelder, 2014; White and Swartzwelder, 2004), the enduring effects of AIE on memory and hippocampal function are of particular interest. Previous studies have shown that AIE alters hippocampal synaptic function and plasticity (Sabeti and Gruol, 2008), but those studies did not address whether the effects of AIE persist into adulthood. Studies of the more enduring effects of AIE have shown impairment of spatial learning (Sircar and Sircar, 2005) and retention of

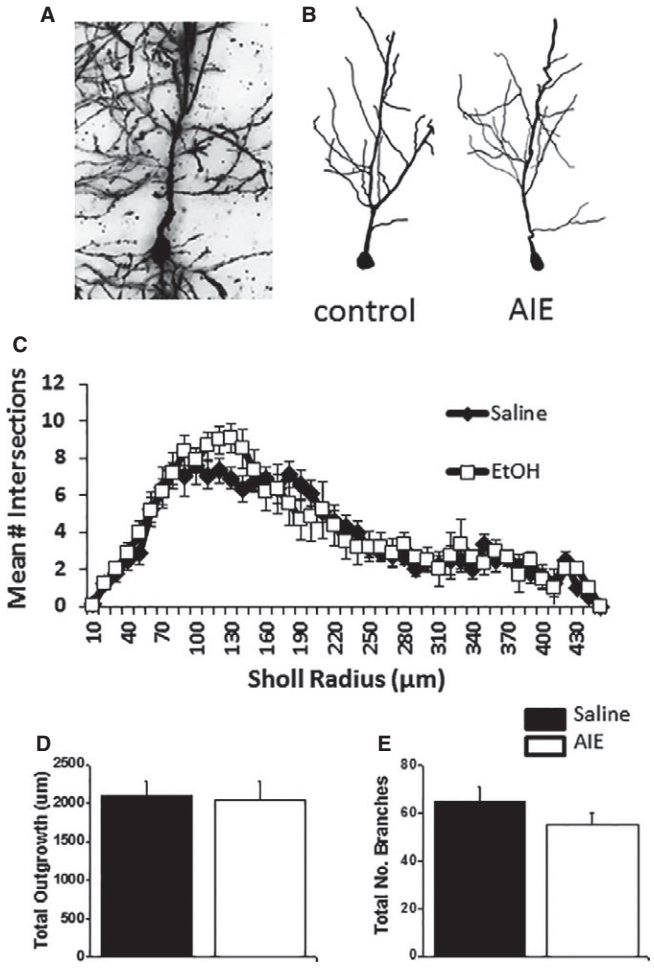

Fig. 5. Adolescent intermittent ethanol (AIE) does not alter dendritic arborization in CA1 hippocampal neurons. High power image (**A**) and Neurolucida tracing reconstructions (**B**) corresponding to representative CA1 pyramidal neurons from saline- and AIE-treated rats (scale bar, 50 μm). Sholl analysis showing the mean number of intersections that cross 10-μm radii intervals showed no significant differences between treatment groups ($p = 0.618$; **C**). There were also no significant differences in total outgrowth or dendritic branch number ($p = 0.434$, $p = 0.126$, (**D** and **E**), respectively). Data represent the mean ± SEM from the following number of neurons: saline ($n = 11$), AIE ($n = 10$).

fear conditioning (Broadwater and Spear, 2013) several weeks after the termination of EtOH treatment, suggesting that hippocampal function may be altered in a similarly enduring timeline. Therefore, we measured LTP, dendritic spine morphology, and synaptic structure in hippocampal area CA1. We found that AIE increased the likelihood of LTP at a low stimulus intensity that was insufficient to induce LTP in slices from control animals, reminiscent of the propensity toward LTP induction by mild stimulus trains in the adolescent hippocampus (Swartzwelder et al., 1995; Teyler et al., 1988). Synaptic immaturity after AIE was also indicated by Golgi analysis, which revealed an increase in the number of immature dendritic spines and a decrease in the number of mature spines. Immunohistochemistry indicated that AIE diminished the number of VGlut1/PSD-95 and VGlut1/SAP102 co-localized synaptic puncta. These effects were driven by decreases in the postsynaptic markers, PSD-95 and SAP102, in the absence of an effect on presynaptic VGlut1.

The increase in LTP induction that we observed after AIE may be secondary to an imbalance of inhibitory/excitatory mechanisms. This is important because EtOH affects both excitatory and inhibitory neuronal activity. In particular, extrasynaptic $GABA_A$ receptors have been shown to be highly sensitive to EtOH (Wallner et al., 2003), and we recently showed that AIE reduced tonic inhibition in dentate granule cells from adult rats to levels typically seen in adolescents (Fleming et al., 2013). We have also determined that the $GABA_A$ delta receptor subunit, which drives tonic inhibition, is significantly reduced after AIE in whole hippocampal samples (Centanni et al., 2014). Further work will be necessary to determine whether these changes in tonic inhibition are driving excitatory changes within the CA1 network. However, it is feasible that the AIE-induced LTP changes observed here could be due to changes in the excitatory/inhibitory balance in the neuronal circuits within CA1.

Enhanced plasticity of this type has been associated with memory deficits and other neuropsychological impairments (Zorumski and Izumi, 2012). Additionally, the biasing of neural circuits toward excitatory synaptic plasticity has been associated with neurotoxic liability (Olney, 1969), neuronal death (Cull-Candy et al., 2001), and the occlusion of memory-related synaptic function (Moser et al., 1998). Thus, the enhanced LTP induction that we observed after AIE could reflect enhanced metaplasticity in hippocampal circuits and predispose animals to deficits in hippocampally mediated learning and memory dysfunction.

Our observation of an AIE-induced increase in immature-like dendritic spines in adulthood is intriguing in the context of the observed changes in LTP induction. As overexpression of PSD-95 has been shown to promote dendritic spine maturation and changes in dendritic morphology (Béïque et al., 2006; El-Husseini et al., 2000; Zheng et al., 2012), we hypothesized that AIE would also result in a decrease in PSD-95, leading to the retention of this immature-like dendritic spine phenotype in adulthood (El-Husseini et al., 2000; Zheng et al., 2012). Also, if these dendritic spines were truly immature, and not just abnormal, they would contain more SAP102: a PSD protein typically seen in immature spines that can compensate for reductions in PSD-95 (Bonnet et al., 2013). Although we found a reduction in PSD-95, indicative of immaturity, we also found a reduction in SAP102. These findings are important because changes in these PSD proteins have previously been associated with changes in spine morphology typically observed in neurodevelopmental disorders (Tarpey et al., 2004; Zanni et al., 2010) and could influence receptor insertion. Thus, these structural changes may reflect an underlying spine abnormality that is not necessarily or exclusively related to functional immaturity.

In conclusion, these experiments demonstrate that the adolescent hippocampus is vulnerable to EtOH-induced neuronal insult, the sequelae of which last into adulthood

and include morphological changes, alterations in memory-related synaptic plasticity, and the expression of postsynaptic MAGUKs. These findings support the emerging hypothesis that AIE induces an array of pathological neural changes that can manifest with immature-like characteristics into adulthood.

ACKNOWLEDGMENTS

Many thanks to Dana Morin, Hannah Sexton, Jennifer Bourne, Jonnathan Singh Alvarado, and Alexander Alvarado Singh for their technical support. Thanks to Lesa Hall for the artwork. The work was supported by U01AA019925 NADIA (to HSS), UO1AA020938 and BX-001271-02 (to SDM), DA031833 (to CE), 2T32NS51156-6 and 1F32NS0 83283-01A1 (to WCR), U.S. Department of Veterans Affairs, Senior Research Career Scientist award (to HSS), BX-002128-01 (to RLF), VA CDAs IK2BX001267 (to SKA) and 2-010-10S (to RLF), Institute for Medical Research (to RCK), DVAMC VSN 6 MIRECC (to SDM and RCK), and K99-AA22651 (to TW). CE was an Esther and Joseph Klingenstein Fund Fellow and Alfred P. Sloan Fellow.

REFERENCES

Acheson SK, Bearison C, Risher ML, Abdelwahab SH, Wilson WA, Swartzwelder HS (2012) Effects of acute or chronic ethanol exposure during adolescence on behavioral inhibition and efficiency in a modified water maze task. PLoS ONE 8:1–15.

Béïque J-C, Lin D-T, Kang M-G, Aizawa H, Takamiya K, Huganir R (2006) Synapse-specific regulation of AMPA receptor function by PSD-95. Proc Natl Acad Sci USA 103:19535–19540.

Bonnet SA, Akad DS, Samaddar T, Liu Y, Huang X, Dong Y, Schlüter OM (2013) Synaptic state-dependent functional interplay between postsynaptic density-95 and synapse-associated protein 102. J Neurosci 33:13398–13409.

Bourne J, Harris K (2007) Do thin spines learn to be mushroom spines that remember? Curr Opin Neurobiol 17:381–386.

Bourne J, Harris K (2008) Balancing structure and function at hippocampal dendritic spines. Annu Rev Neurosci 31:47–67.

Bourne J, Harris K (2011) Coordination of size and number of excitatory and inhibitory synapses results in a balanced structural plasticity along mature hippocampal CA1 dendrites during LTP. Hippocampus 21:354–373.

Broadwater M, Spear LP (2013) Consequences of ethanol exposure on cued and contextual fear conditioning and extinction differ depending on timing of exposure during adolescence or adulthood. Behav Brain Res 256:10–19.

Brown S, Tapert S, Granholm E, Delis D (2000) Neurocognitive functioning of adolescents: effects of protracted alcohol use. Alcohol Clin Exp Res 24:164–171.

Brun VH, Ytterbo K, Morris RG, Moser MB, Moser EI (2001) Retrograde amnesia for spatial memory induced by NMDA receptor-mediated long-term potentiation. J Neurosci 21:356–362.

Centanni SW, Teppen T, Risher ML, Fleming RL, Moss JL, Acheson SK, Mulholland PJ, Pandey SC, Chandler LJ, Swartzwelder HS (2014) Adolescent alcohol exposure alters GABAA receptor subunit expression in adult hippocampus. Alcohol Clin Exp Res 38:2800–2808.

Choudhury S, Blakemore S-J, Charman T (2006) Social cognitive development during adolescence. Soc Cogn Affect Neurosci 1:165–174.

Cull-Candy S, Brickley S, Farrant M (2001) NMDA receptor subunits: diversity, development and disease. Curr Opin Neurobiol 11:327–335.

Diaz-Granados J, Graham D (2007) The effects of continuous and intermittent ethanol exposure in adolesence on the aversive properties of ethanol during adulthood. Alcohol Clin Exp Res 31:2020–2027.

El-Husseini A, Schnell E, Chetkovich D, Nicoll R, Bredt D (2000) PSD-95 involvement in maturation of excitatory synapses. Science 290:1364–1368.

Elias GM, Elias LA, Apostolides PF, Kriegstein AR, Nicoll RA (2008) Differential trafficking of AMPA and NMDA receptors by SAP102 and PSD-95 underlies synapse development. Proc Natl Acad Sci USA 105:20953–20958.

Fiala JC (2005) Reconstruct: a free editor for serial section microscopy. J Microsc 218:52–61.

Fleming R, Acheson S, Moore S, Wilson W, Swartzwelder H (2012) In the rat, chronic intermittent ethanol exposure during adolescence alters the ethanol sensitivity of tonic inhibition in adulthood. Alcohol Clin Exp Res 36:279–285.

Fleming R, Li Q, Risher M-L, Sexton H, Moore S, Wilson W, Acheson S, Swartzwelder H (2013) Binge-pattern ethanol exposure during adolescence, but not adulthood, causes persistent changes in GABAA receptor-mediated tonic inhibition in dentate granule cells. Alcohol Clin Exp Res 37:1154–1160.

Hanson K, Medina K, Padula C, Tapert S, Brown S (2011) Impact of adolescent alcohol and drug use on neuropsychological functioning in young adulthood: 10-year outcomes. J Child Adolesc Subst Abuse 20:135–154.

Ippolito D, Eroglu C (2010) Quantifying synapses: an immunocytochemistry-based assay to quantify synapse number. J Vis Exp 45: 1–8.

Kilb W (2012) Development of the GABAergic system from birth to adolescence. Neuroscientist 18:613–630.

Klein RC, Saini S, Risher M-L, Acheson SK, Fleming RL, Sexton HG, Swartzwelder HS, Moore SD (2014) Regional-specific effects of ovarian hormone loss on synaptic plasticity in adult human APOE targeted replacement mice. PLoS ONE 9:e94071.

Li Q, Fleming R, Acheson S, Madison R, Moore S, Risher M-L, Wilson W, Swarztwelder H (2013) Long-term modulation of A-type K(+) conductances in hippocampal CA1 interneurons in rats after chronic intermittent ethanol exposure during adolescence or adulthood. Alcohol Clin Exp Res 37:2074–2085.

Little P, Kuhn C, Wilson W, Swartzwelder H (1996) Differential effects of ethanol in adolescent and adult rats. Alcohol Clin Exp Res 20:1346–1351.

Markwiese B, Acheson S, Levin E, Wilson W, Swartzwelder H (1998) Differential effects of ethanol on memory in adolescent and adult rats. Alcohol Clin Exp Res 22:416–421.

Matsuzaki M (2007) Factors critical for the plasticity of dendritic spines and memory storage. Neurosci Res 57:1–9.

Matthews D, Tinsley K, Diaz-Granados J, Tokunaga S, Silvers J (2008) Chronic intermittent exposure to ethanol during adolescence produces tolerance to the hypnotic effects of ethanol in male rats: a dose-dependent analysis. Alcohol 42: 617–621.

Moser E, Krobert K, Moser M, Morris R (1998) Impaired spatial learning after saturation of long-term potentiation. Science 281:2038–2042.

NIAAA (2004) NIAAA council approves definition of binge drinking. NIAAA Newsletter . Available at: http://pubs.niaaa.nih.gov/publications/Newsletter/winter2004/Newsletter_Number3.pdf. Accessed April 12, 2015.

Olney J (1969) Brain lesions, obesity, and other disturbances in mice treated with monosodium glutamate. Science 164:719–721.

Paus T (2005) Mapping brain maturation and cognitive development during adolescence. Trends Cogn Sci 9:60–68.

Risher M-L, Fleming R, Boutros N, Semenova S, Wilson W, Levin E, Markou A, Swartzwelder H, Acheson S (2013) Long-term effects of chronic intermittent ethanol exposure in adolescent and adult rats: radial-arm maze performance and operant food reinforced responding. PLoS ONE 8: e62940.

Risher WC, Ustunkaya T, Singh Alvarado J, Eroglu C (2014) Rapid Golgi analysis method for efficient and unbiased classification of dendritic spines. PLoS ONE 9:1–8.

Sabeti J, Gruol D (2008) Emergence of NMDAR-independent long-term potentiation at hippocampal CA1 synapses following early adolescent

exposure to chronic intermittent ethanol: role for sigma-receptors. Hippocampus 18:148–168.

Silvers JM, Tokunaga S, Mittleman G, Matthews DB (2003) Chronic intermittent injections of high-dose ethanol during adolescence produces metabolic, hypnotic, and cognitive tolerance in rats. Alcohol Clin Exp Res 27:1606–1612.

Silvers JM, Tokunaga S, Mittleman G, O'Buckley T, Morrow AL, Matthews DB (2006) Chronic intermittent ethanol exposure during adolescence reduces the effect of ethanol challenge on hippocampal allopregnanolone levels and Morris water maze task performance. Alcohol 39:151–158.

Sircar R, Sircar D (2005) Adolescent rats exposed to repeated ethanol treatments show lingering behavioral impairments. Alcohol Clin Exp Res 29:1402–1410.

Spear L (2000) The adolescent brain and age-related behavioral manifestations. Neurosci Biobehav Rev 24:417–463.

Spear LP, Swartzwelder HS (2014) Adolescent alcohol exposure and persistence of adolescent-typical phenotypes into adulthood: a mini-review. Neurosci Biobehav Rev 45:1–8.

Squeglia LM, Pulido C, Wetherill RR, Jacobus J, Brown GG, Tapert SF (2012) Brain response to working memory over three years of adolescence: influence of initiating heavy drinking. J Stud Alcohol Drugs 73:749.

Swartzwelder H, Wilson W, Tayyeb M (1995) Age-dependent inhibition of long-term potentiation by ethanol in immature versus mature hippocampus. Alcohol Clin Exp Res 19:1480–1485.

Tada T, Sheng M (2006) Molecular mechanisms of dendritic spine morphogenesis. Curr Opin Neurobiol 16:95101.

Tarpey P, Parnau J, Blow M, Woffendin H, Bignell G, Cox C, Cox J, Davies H, Edkins S, Holden S, Korny A, Mallya U, Moon J, O'Meara S, Parker A, Stephens P, Stevens C, Teague J, Donnelly A, Mangelsdorf M, Mulley J, Partington M, Turner G, Stevenson R, Schwartz C, Young I, Easton D, Bobrow M, Futreal PA, Stratton MR, Gecz J, Wooster R, Raymond FL (2004) Mutations in the DLG3 gene cause nonsyndromic X-linked mental retardation. Am J Hum Genet 75:318–324.

Teyler TJ, Perkins AT, Harris KM (1988) The development of long-term potentiation in hippocampus and neocortex. Neuropsychologia 27:31–39.

Wallner M, Hanchar HJ, Olsen RW (2003) Ethanol enhances $\alpha 4\beta 3\sigma$ and $\alpha 6\beta 3\sigma$ Υ-aminobutyric acid type A receptors at low concentrations known to affect humans. Proc Natl Acad Sci USA 100: 1518–1523.

White A, Ghia A, Levin E, Swartzwelder H (2000) Binge pattern ethanol exposure in adolescent and adult rats: differential impact on subsequent responsiveness to ethanol. Alcohol Clin Exp Res 24: 1251–1256.

White AM, Swartzwelder HS (2004) Hippocampal function during adolescence: a unique target of ethanol effects. Ann N Y Acad Sci 1021:206–220.

Yuste R (2009) Dendritic Spines. MIT Press Books, Cambridge, MA.

Zanni G, van Esch H, Bensalem A, Saillour Y, Poirier K, Castelnau L, Ropers HH, de Brouwer AP, Laumonnier F, Fryns J-PP, Chelly J (2010) A novel mutation in the DLG3 gene encoding the synapse-associated protein 102 (SAP102) causes non-syndromic mental retardation. Neurogenetics 11:251–255.

Zheng S, Gray E, Chawla G, Porse B, O'Dell T, Black D (2012) PSD-95 is post-transcriptionally repressed during early neural development by PTBP1 and PTBP2. Nat Neurosci 15:381–388, S1.

Zorumski C, Izumi Y (2012) NMDA receptors and metaplasticity: mechanisms and possible roles in neuropsychiatric disorders. Neurosci Biobehav Rev 36:989–1000.